

Tensor network representations of fermionic crystalline topological phases on two-dimensional lattices

Jian-Hao Zhang^{1,*} and Shuo Yang^{2,3,†}

¹*Department of Physics, The Chinese University of Hong Kong, Shatin, New Territories, Hong Kong, China*

²*State Key Laboratory of Low Dimensional Quantum Physics and
Department of Physics, Tsinghua University, Beijing 100084, China*

³*Frontier Science Center for Quantum Information, Beijing 100084, China*

We investigate the tensor network representations of fermionic crystalline symmetry-protected topological (SPT) phases on two-dimensional lattices. As a mapping from virtual indices to physical indices, projected entangled-pair state (PEPS) serves as a concrete way to construct the wavefunctions of 2D crystalline fermionic SPT (fSPT) phases protected by 17 wallpaper group symmetries, for both spinless and spin-1/2 fermions. Based on PEPS, the full classification of 2D crystalline fSPT phases with wallpaper groups can be obtained. Tensor network states provide a natural framework for studying 2D crystalline fSPT phases.

CONTENTS

I. Introduction	1
II. Tensor networks with the graded structure on the 2D lattice	2
A. Virtual indices without symmetry	4
B. Virtual indices with reflection symmetry	4
C. The role of translation symmetry	4
III. General paradigm of classifying crystalline SPT phases	5
IV. An explicit example of crystalline fSPT phases	5
A. Spinless fermions	6
B. Spin-1/2 fermions	8
V. Conclusion and discussion	9
Acknowledgments	10
A. Group extension, the spin of fermions and short exact sequence	10
1. Central extension of groups	11
2. Physical understanding of spin of fermions	11
B. Physical indices in 2D systems	12
C. Superposition of MPOs with graded structure	13
1. Superposition of bMPOs	13
a. Superpositions of three bMPOs: F -move	13
b. Superpositions of four bMPOs: Pentagon equation	13
2. Superposition of fMPOs	13
References	15

I. INTRODUCTION

Since the discovery of Haldane phase in one-dimensional spin chain [1, 2], the interplay between symmetry and topology has been one of the most crucial issues in condensed matter physics during the past few decades. Representative examples including topological insulators (TI) and superconductors (TSC) have been intensively studied theoretically and experimentally [3, 4]. In recent years, a large class of nontrivial topological phases require symmetry protections: they can be smoothly deformed to a trivial phase in the absence of global symmetry. Such symmetry-protected topological (SPT) phases are systematically constructed and classified [5–45] in both interacting bosonic and fermionic systems.

On the other hand, tensor networks are extremely suitable for describing SPT phases because nonlocal topological characters of a system are captured by the symmetries of local tensors [6, 46–57]. In one-dimensional (1D) systems, all SPT states can be constructed and classified by matrix product state (MPS). In 2D systems, bosonic SPT (bSPT) phases are constructed by projected entangled-pair states (PEPS) and classified by matrix product operators (MPO) acting on arbitrary boundary of PEPS; fermionic SPT (fSPT) phases are constructed by PEPS with graded structure who characterizes the fermion parity.

In recent years, crystalline symmetry plays a more important role in studying SPT phases because each monocrystal in condensed matter systems corresponds to a specific space group in arbitrary dimension. Crystalline SPT phases are not only of conceptual importance [58–81] but also have a great possibility to be experimentally realized. As the simplest example of crystalline SPT phases, the crystalline TI is first proposed in free fermion systems and then be realized in many different materials [82–85]. For free fermion systems, the crystalline SPT phases are systematically constructed and classified by *symmetry indicators*, which are roughly the symmetry representations of band structures at high-symmetry

* jianhaozhang1@cuhk.edu.hk

† shuoyang@tsinghua.edu.cn

momenta. In interacting bosonic and fermionic systems, a systematic *real-space construction* is established by decorating different phases on lower-dimensional blocks [61, 72, 86, 87]. Furthermore, it was pointed out that the classification of crystalline SPT phases are closely related to the SPT phases with internal symmetries. In Ref. [63], a “*crystalline equivalence principle*” is proposed with rigorous mathematical proof: crystalline topological phases with space group symmetry G are in one-to-one correspondence with topological phases protected by the same internal symmetry G but acting in a twisted way. If an element of G is a mirror reflection (orientation-reversing symmetry), it should be regarded as time-reversal symmetry (anti-unitary symmetry). This principle has been confirmed in bosonic [72] and 2D interacting fermionic systems [86, 87].

In this paper, we apply the tensor network method as a more straightforward and comprehensible way to characterize the crystalline fSPT phases in 2D interacting fermionic systems for both spinless and spin-1/2 fermions. Firstly we define PEPS tensors with graded structures on 2D lattices with wallpaper group symmetry as maps from virtual indices to physical indices, where physical/virtual indices are aligned on vertices/links of 2D lattices. Distinct from the systems with on-site symmetry, the local symmetry of physical and virtual indices might be different in crystalline SPT states. Subsequently, by investigating the virtual indices and physical indices of fermionic MPOs (fMPOs), we obtain all classification data as possible PEPS tensors on the lattice. Then by utilizing the injectivity condition, some PEPS tensors may not be well-defined and some others may correspond to trivial SPT phases, we call them *obstruction* and *trivialization*. An obstruction and trivialization-free PEPS corresponds to a nontrivial 2D crystalline fSPT state, and all of them form the classification group. We use the lattice with #9 wallpaper group ($cm\bar{m}$) symmetry as a representative example to highlight this paradigm. Finally, there might be some superposition rules of PEPS tensors, which leads to a nontrivial group structure of the classification of 2D crystalline fSPT phases. According to this paradigm, we obtain the full classifications of 2D crystalline fSPT phases with wallpaper group symmetries (see Table I), confirmed to the results in Refs. [87] and [88] which are yielded by alternative methods (real-space construction and Atiyah-Hirzebruch spectral sequence [89]).

Tensor network is a powerful tool not only for directly constructing the PEPSs as the explicit ground states of crystalline fSPT phases, but also for studying quantum phase transitions between different topological phases. Therefore, constructing tensor network representations of crystalline fSPT phases lays the important foundation for investigating the topological quantum phase transitions of crystalline fSPT phases.

The rest of the paper is organized as follows: In Sec. II, we review the tensor networks with graded structures for describing interacting fermionic states and their appli-

cation to 2D lattices with wallpaper group symmetries. In Sec. III, we introduce the general paradigm of constructing the PEPS tensor network representations of 2D crystalline fSPT states. In Sec. IV, we explicitly construct the PEPS tensor network states of 2D crystalline fSPT phases with #9 wallpaper group symmetry $cm\bar{m}$ as a concrete example, for both spinless and spin-1/2 fermions. All results are summarized in Table I. Finally, the conclusions and discussions about further applications of tensor network representations of 2D crystalline fSPT phases are presented in Sec. V. In Appendix A, we review the mathematical characterization and physical meaning of spins of fermions. In Appendix B, we summarize all possible physical indices of PEPS tensors we might use. All physical indices should be aligned at the center of a specific point group. In Appendix C, we review the superposition and pentagon equation fMPOs with graded structure.

II. TENSOR NETWORKS WITH THE GRADED STRUCTURE ON THE 2D LATTICE

For fermionic systems, the fermion parity is always conserved and is described by the fermion parity symmetry \mathbb{Z}_2^f . To describe this symmetry, we should consider the tensor networks with the graded structure [54]: A super vector space V has a natural direct sum structure:

$$V = V^0 \oplus V^1 \quad (1)$$

where vectors in V^0 and V^1 are called homogeneous vectors, the vector $v \in V^0/V^1$ is said to have even/odd fermion parity.

A 2D PEPS can be defined on any lattice Γ :

$$A_\mu = \sum_{\mu=1}^d \sum_{\{\tau_j\}=1}^{\{D_j\}} (A_\mu)_{\{\tau_j\}}^\mu |\mu\rangle \bigotimes_{\tau_j \in E_\mu} (\tau_j | \quad (2)$$

for $\forall \mu \in \Gamma$. E_μ is the set of edges with μ as an endpoint. Here μ is the physical index running over the basis for the Hilbert space of a site \mathbb{C}^d , and τ_j is the virtual index of dimension D_j along with the bond τ_j , see Fig. 1(a).

Then consider a region $R \in \Gamma$ whose boundary ∂R forms a contractible closed loop. Then we can define a PEPS map in this region as:

$$A_R = \bigotimes_{\tau_j \in \partial R} \mathbb{C}^{D_j} \rightarrow \bigotimes_{\mu_k \in R} \mathbb{C}^{d_k} \quad (3)$$

Here τ_j is the virtual index across ∂R of dimension D_j , and μ_k is the physical index inside the region R of dimension d_k , see Fig. 1(b). We depict that the region R includes an integer number of unit cells.

We note that the PEPS on the lattice with wallpaper group symmetry is slightly different from the PEPS with on-site symmetry. For PEPS with on-site symmetry, the symmetry groups on both physical and virtual indices are

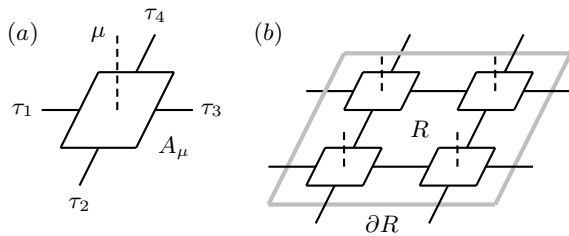


FIG. 1. (a). A PEPS tensor on a quadrate vertex; (b). The PEPS map A_R from virtual indices on edges in ∂R (the boundary of the region R) to the physical indices on vertices in R .

identical; for PEPS on the lattice with wallpaper group symmetry, the symmetry groups on physical indices and virtual indices might be different. This is because the “on-site” symmetry groups of physical and virtual indices are given by the wallpaper group symmetry acting internally. We label the effective “on-site” symmetry of physical/virtual indices by G_p and G_v , respectively. Usually $G_v \subset G_p$.

In order to describe the crystalline SPT phases, we should consider the MPO-injective PEPS with single-blocked condition [52, 57]. Then for PEPS A_{μ_k} on the lattice site μ_k with virtual indices τ_j [$j = 1, 2, 3, 4$, see Fig. 1(a)], there are some subtleties for investigating the invariances under wallpaper group that all come from the difference between the effective “on-site” symmetry on physical and virtual indices ($G_p \neq G_v$). For example, we suppose the PEPS indicated in Fig. 1(a) is assigned on the lattice site as the center of 2-order dihedral group symmetry D_2 which is generated by two reflection symmetry generators \mathbf{M}_1 and \mathbf{M}_2 . Some of the virtual indices might be related by operations $g \in D_2$:

$$\begin{aligned} \mathbf{M}_1 : (\tau_1, \tau_2, \tau_3, \tau_4) &\mapsto (\tau_1, \tau_4, \tau_3, \tau_2) \\ \mathbf{M}_2 : (\tau_1, \tau_2, \tau_3, \tau_4) &\mapsto (\tau_3, \tau_2, \tau_1, \tau_4) \end{aligned} \quad (4)$$

Hence the effective “on-site” symmetries of physical/virtual indices are $G_p = \mathbb{Z}_2 \rtimes \mathbb{Z}_2$, $G_v = \mathbb{Z}_2$ (for virtual indices τ_1 and τ_3 , \mathbf{M}_1 acts internally; for virtual indices τ_2 and τ_4 , \mathbf{M}_2 acts internally). In fact, we have the following short exact sequence:

$$0 \rightarrow G_v \rightarrow G_p \rightarrow G_p/G_v \rightarrow 0 \quad (5)$$

For $\forall g \in G_p$, we can express it in terms of a product of two group elements: $g = g_0 h$, where $g_0 \in G_v$ acts on the virtual indices internally, and $h \in G_p/G_v$ transforms a virtual index to another.

The graded structure of the physical indices is characterized by a map $n_1 : G_p \rightarrow \mathbb{Z}_2 = \{0, 1\}$ and classified by 1-cohomology $\mathcal{H}^1(G_p, \mathbb{Z}_2)$; The graded structure of the virtual indices is characterized by another map $n_2 : G_v \times G_v \rightarrow \mathbb{Z}_2 = \{0, 1\}$ and classified by 2-cohomology $\mathcal{H}^2(G_v, \mathbb{Z}_2)$. This is because a virtual bond always connects two virtual degrees of freedom, but a

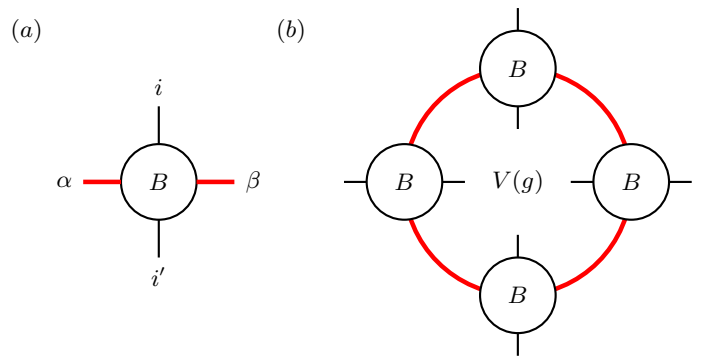


FIG. 2. Graphical representation of (a). An MPO tensor; (b). The MPO symmetry operator $V(g)$ on the virtual indices connected to the lattice site μ . Solid black/red links label the virtual indices of PEPSs/MPOs.

physical bond is only relevant to a single degree of freedom at the lattice site. Furthermore, the fermion parity of each PEPS tensor should be even (because the fermion parity symmetry cannot be broken under any morphisms, such as A_μ), hence the above maps to \mathbb{Z}_2 , n_1 and n_2 are 1-cocycle/2-cocycle [54].

With the aforementioned arguments, we are ready to investigate the wallpaper group symmetry properties on PEPS. Firstly we consider the PEPS A_μ on a single lattice site μ , as indicated in Fig. 1(a). Physical symmetry acting on the physical index should form a linear representation of G_p with the notation $U(g)$, $g \in G_p$. On the virtual indices, the symmetry action $V(g)$ is a fermionic matrix product operator (fMPO) acting on the virtual indices. Repeatedly because $G_v \neq G_p$, The fMPO for wallpaper group symmetry is slightly different from the cases with on-site symmetry. The MPO $V(g)$ associated with the PEPS we discussed in this paragraph is:

$$\begin{aligned} V(g) = \sum_{\{i_n\}=1}^{\{D_n\}} \sum_{\{i'_n\}=1}^{\{D_n\}} \text{Tr} \left[B_{\tau_1}^{i_1, i'_1} B_{\tau_2}^{i_2, i'_2} B_{\tau_3}^{i_3, i'_3} B_{\tau_4}^{i_4, i'_4} \right] \\ \times |i_1, i_2, i_3, i_4\rangle \langle i'_1, i'_2, i'_3, i'_4| \end{aligned} \quad (6)$$

where D_n is the dimension of the virtual index τ_n (might be different for various n), and $(B_{\tau}^{i, i'})_{a, b}$ is a $\chi \times \chi$ matrix, as shown in Fig. 2. Hence the symmetry of the PEPS A_μ is of the form:

$$U(g)A_\mu = A_\mu V(g) \quad (7)$$

In general, for the region $R \in \Gamma$, The symmetry of the PEPS A_R is of the form:

$$\bigotimes_{\mu_k \in R} U_k(g_k)A_R = A_R V^{\partial R} \quad (8)$$

where $g_k \in G_p^{\mu_k}$ is a group element of the symmetry acting on the lattice site μ_k internally, U_k is the corresponding linear representation; the fMPO $V^{\partial R}$ is of the

form:

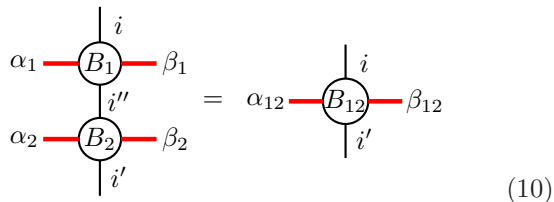
$$V^{\partial R} = \sum_{\{i_n\}=1}^{\{D_n\}} \sum_{\{i'_n\}=1}^{\{D_n\}} \text{Tr} \left[B_{\tau_1}^{i_1, i'_1} \cdots B_{\tau_N}^{i_N, i'_N} \right] \times |i_1, \dots, i_N\rangle \langle i'_1, \dots, i'_N| \quad (9)$$

where the virtual indices crossing ∂R are ordered from 1 to $N = |\partial R|_e$ (the number of virtual indices crossing ∂R).

A unique property of the 2D lattice with wallpaper group symmetry is that there is only one possible symmetry operation acting on the bond of lattice, i.e., the reflection symmetry operation. Equivalently, the effective “on-site” symmetry of the virtual indices G_v is either no or \mathbb{Z}_2 . We will discuss them separately.

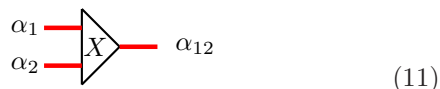
A. Virtual indices without symmetry

For the virtual index crossing ∂R without effective “on-site” symmetry, the connecting fermionic MPO (fMPO) can be illustrated as Fig. 2(a). Superposing two fMPOs gives a new fMPO, with the following graphical representation:



$$\begin{array}{c} \alpha_1 \text{---} B_1 \text{---} \beta_1 \\ | \\ i \\ | \\ \alpha_2 \text{---} B_2 \text{---} \beta_2 \\ | \\ i'' \\ | \\ i' \end{array} = \begin{array}{c} \alpha_{12} \text{---} B_{12} \text{---} \beta_{12} \\ | \\ i \\ | \\ i' \end{array} \quad (10)$$

This can be realized by defining a projection operator with the graded structure (see Appendix C for more details):



$$\begin{array}{c} \alpha_1 \\ \alpha_2 \end{array} \text{---} \triangle X \text{---} \alpha_{12} \quad (11)$$

In Appendix C, we note that for the translation symmetry breaking system with on-site symmetry G , the different fSPT phases are labeled by 3-order group supercohomology with the following indices:

$$\begin{cases} n_1 \in \mathcal{H}^1(G, \mathbb{Z}_2) \\ n_2 \in \mathcal{H}^2(G, \mathbb{Z}_2) \\ \nu_3 \in \mathcal{H}^3[G, U(1)] \end{cases} \quad (12)$$

which are given by the F -moves and super pentagon equations of the fMPOs with graded structure. Nevertheless, for arbitrary indices connected a fMPO as indicated in Fig. 2(a), there is no effective “on-site” symmetry. As the consequence, all parameters (n_1, n_2, ν_3) in Eq. (12) are trivial.

B. Virtual indices with reflection symmetry

For the virtual index crossing ∂R at which the reflection symmetry acting internally, the connecting fMPO can still be illustrated as Fig. 2(a). We demonstrate that there is a subtle difference between the true \mathbb{Z}_2 on-site symmetry and the reflection symmetry acting internally. Here the virtual indices i and i' are aligned on the reflection axis, and the reflection symmetry operation exchanges the indices α and β . Equivalently, there is no effective “on-site” symmetry on the indices α and β which is distinct from the case with true \mathbb{Z}_2 on-site symmetry.

The superposition of fMPOs for this case can still be described by Eq. (10) and realized by the projection operator defined in Eq. (C2). Nevertheless, there is no effective “on-site” symmetry on the indices α and β , hence all parameters in Eq. (12) are also trivial.

We conclude that the fMPOs connected to ∂R do not give rise to any nontrivial fSPT phases for both cases (with and without reflection symmetry).

C. The role of translation symmetry

In Ref. 6 the authors demonstrated that for a bosonic system, each virtual bond in Fig. 1 represents an entanglement pair between a projective representation of the symmetry group G and its inverse that is classified by 2-cohomology $\mathcal{H}^2[G, U(1)]$. For a fermionic system, each virtual bond has a graded structure representing the fermion parity which is classified by 1-cohomology $\mathcal{H}^1(G, \mathbb{Z}_2)$; furthermore, the virtual bond in a fermionic system can also represent the Majorana entanglement pair (MEP) that is formed by two Majorana fermions γ_1 and γ_2 : $i\gamma_1\gamma_2$ [20, 21, 90, 91] which contribute another \mathbb{Z}_2 . Therefore, the virtual indices of the PEPS tensor in the fermionic systems are characterized by the following three parameters:

$$\begin{cases} n_0 \in \mathbb{Z}_2 = \mathcal{H}^0(G, \mathbb{Z}_2) \\ n_1 \in \mathcal{H}^1(G, \mathbb{Z}_2) \\ \nu_2 \in \mathcal{H}^2[G, U(1)] \end{cases} \quad (13)$$

with twisted cocycle conditions [15–17] ($g_1, g_2, g_3 \in G$):

$$\begin{aligned} n_1(g_1) + n_1(g_2) - n_1(g_1g_2) &= \omega_2 \smile n_0 \\ \frac{\nu_2(g_1, g_2)\nu_2(g_1g_2, g_3)}{\nu_2(g_1, g_2g_3)\nu_2(g_2, g_3)} &= (-1)^{\omega_2 \smile n_1(g_1, g_2, g_3)} \end{aligned} \quad (14)$$

Therefore, if we truncate all virtual bonds crossing ∂R , there is an unpaired dangling mode characterized by parameters (n_0, n_1, ν_2) [cf. Eq. (13)] on each virtual bond crossing ∂R , with the effective “on-site” symmetry group $G_v = 0$ or \mathbb{Z}_2 [92].

With the absence of translation symmetry, boundary modes can be combined by renormalization and change the parameters (n_0, n_1, ν_2) from one to another and, in

particular, to the trivial class. On the other hand, if we restore the translation symmetry, each boundary mode is well-defined. The parameters (n_0, n_1, ν_2) do label different phases because the renormalization procedure breaks the translation symmetry.

III. GENERAL PARADIGM OF CLASSIFYING CRYSTALLINE SPT PHASES

In this section, we highlight the general paradigm of the classification of the crystalline fSPT phases on 2D lattice with wallpaper group symmetry. There are several major steps:

1. The physical indices with graded structure: consider a 2D PEPS tensor network state on a torus who has no open virtual index (because of the absence of the boundary) with translation symmetry, a gapped state $|\psi\rangle$ that do not break the two symmetries must transform as $(\forall g \in G_p)$:

$$U(g) \otimes \cdots \otimes U(g)|\psi\rangle = [\alpha(g)]^N \quad (15)$$

Here $U(g)$ is the linear representation of G_p acting on each site, N is the number of PEPS tensor, and $\alpha(g)$ is an 1D linear representation of G_p which is classified by 1-cohomology $\mathcal{H}^1[G_p, U(1)]$. Together with the \mathbb{Z}_2 from graded structure, the physical indices of the fermionic PEPS tensor are characterized by the following two parameters:

$$n_0 \in \mathbb{Z}_2, \quad \nu_1 \in \mathcal{H}^1[G_p, U(1)] \quad (16)$$

with the twisted cocycle conditions [15–17] ($g_1, g_2 \in G_p$):

$$\frac{\nu_1(g_1)\nu_1(g_2)}{\nu_1(g_1g_2)} = (-1)^{\omega_2(g_1, g_2)} \quad (17)$$

Alternatively, these two parameters can be unified to a single 1-cocycle in 1-cohomology of the *total* symmetry group $G_p^f = G_p \times_{\omega_2} \mathbb{Z}_2^f$: $\mathcal{H}^1[G_p^f, U(1)]$. All possible cases for 2D systems are summarized in Appendix B.

2. The virtual indices with graded structure: characterized by Eq. (13) with twisted cocycle conditions (14). For 2D systems, there are only two possibilities: $G_v = \mathbb{Z}_1$ (virtual bond away from reflection axis) or \mathbb{Z}_2 (virtual bond on the reflection axis). For spinless fermions, the virtual bond with $G_v = \mathbb{Z}_1$ has only one nontrivial index: MEP; the virtual bond with $G_v = \mathbb{Z}_2$ has two nontrivial indices: MEP and double MEPs. For spin-1/2 fermions, the virtual bond with $G_v = \mathbb{Z}_1$ has only one nontrivial index: MEP; the virtual bond with $G_v = \mathbb{Z}_2$ does not have any nontrivial index.
3. Obstruction: Each virtual bond connects a dangling mode characterized by Eq. (13) and its inverse. By definition, each PEPS tensor on a lattice site [see Fig.

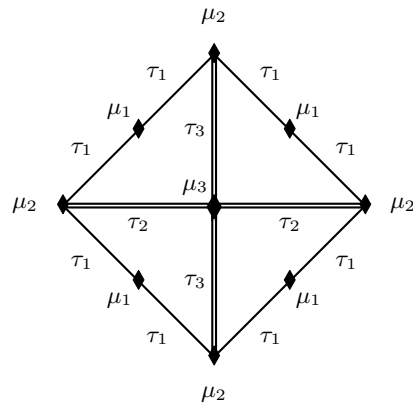


FIG. 3. The unit cell of #9 wallpaper group cmm . Each double solid line represents a reflection axis and each solid diamond represents a center of 2-fold rotation symmetry.

- 1(a)] is a map from the connecting virtual indices to the physical index, hence for a valid SPT phase, the dangling modes at the endpoints of virtual bonds should form a linear representation of G_p^f . If not, we say the corresponding PEPS tensor is *obstructed*.
4. Trivialization: Nontrivial PEPSs do not warrant nontrivial crystalline SPT phases, we should further consider possible trivializations that deform nontrivial PEPSs to trivial states. Some tensor-network states can be mutually deformed by some symmetric finite-depth quantum circuits, hence they are topologically equivalent. Equivalently, trivializations of tensor-network states are characterized by the superposition of PEPS tensors.
5. Group structure of the classification: The accurate group structure of classification will be obtained after investigating the composite rule of different PEPS tensors. More precisely, stacking several copies of a PEPS tensor may leads to another nontrivial PEPS tensor.

IV. AN EXPLICIT EXAMPLE OF CRYSTALLINE FSPT PHASES

With the general paradigm of constructing and classifying the symmetric tensor-network states of crystalline fSPT phases on 2D lattice with wallpaper group symmetry, we demonstrate a concrete and representative example in this section: the crystalline fSPT phases on 2D lattice with #9 wallpaper group symmetry labeled by cmm .

From translation symmetry, the PEPS tensors in different unit cells are identical. Equivalently, it is enough to investigate the PEPS tensors in a specific unit cell. Fig. 3 illustrates the unit cell of cmm symmetry group.

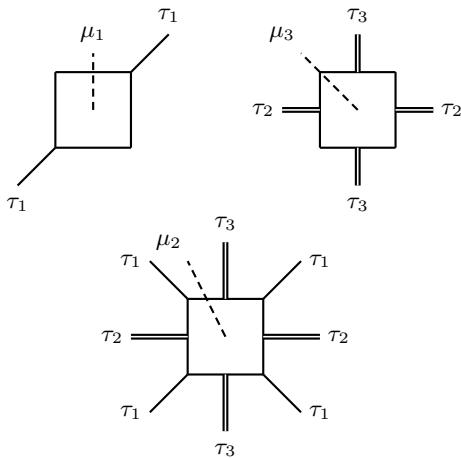


FIG. 4. Independent PEPS tensors A_{μ_j} of cmm symmetric crystalline fSPT phases. μ_j/τ_j represent physical/virtual indices ($j = 1, 2, 3$).

As a consequence, there are only three independent PEPS tensors as illustrated in Fig. 4.

We discuss the spinless fermions and spin-1/2 fermions separately.

A. Spinless fermions

Firstly we investigate the physical indices of A_{μ_j} ($j = 1, 2, 3$) that are characterized by Eqs. (16) and (17). Dimension of the physical index of A_{μ_1} is $d_1 = 4$ with two generators: complex fermion (c) and eigenvalue -1 of 2-fold rotation (r); dimension of the physical index of A_{μ_2}/A_{μ_3} is $d_{2,3} = 8$ with three generators: complex fermion (c) and eigenstates of two reflection generators of D_2 group with eigenvalues -1 (m_1 and m_2).

Subsequently we investigate the virtual indices of A_{μ_j} that are labeled by τ_k ($k = 1, 2, 3$) and characterized by Eqs. (13) and (14). Dimension of τ_1 is $D_1 = 2$ with one generator: MEP [n_0 in Eq. (13)]; dimension of $\tau_{2,3}$ is $D_{2,3} = 4$ with two generators: MEP and double MEPs [n_0 and n_1 in Eq. (13)].

Some of the virtual indices may be obstructed: If there is an MEP on each virtual bond τ_1 , there will be two Majorana fermions at each physical index μ_1 with the following 2-fold rotation property:

$$\mathbf{R} \in C_2 : \gamma_1 \leftrightarrow \gamma_2 \quad (18)$$

Nevertheless, γ_1 and γ_2 form a projective representation of the symmetry group $\mathbb{Z}_2^f \times \mathbb{Z}_2$ on μ_1 : define a complex fermion from γ_1 and γ_2 : $c^\dagger = (\gamma_1 + i\gamma_2)/2$ that span a 2D Hilbert space formed by $|0\rangle$ and $c^\dagger|0\rangle$. In this Hilbert space, $\gamma_1 = \sigma^x$, $\gamma_2 = \sigma^y$, fermion parity operator $P_f = \sigma^z$ and $\mathbf{R} = (\sigma^x + \sigma^y)/\sqrt{2}$, where σ^x , σ^y and σ^z are Pauli matrices. This representation satisfies the spinless condition of fermions: $\mathbf{R}^2 = 1$. It is easy to verify that the fermion parity P_f and 2-fold rotation \mathbf{R}

are anticommute: $P_f \mathbf{R} = -\mathbf{R} P_f$ that is the sufficient condition manifesting that the Hilbert space is a projective representation of $\mathbb{Z}_2^f \times \mathbb{Z}_2$. Accordingly, the MEP on each virtual bond τ_1 is obstructed. Similarly, the MEP on each virtual bond τ_2/τ_3 is obstructed because it leads a projective representation of the local symmetry group $G_{\mu_2}^f/G_{\mu_3}^f$ of the physical index μ_2/μ_3 .

If there are double MEPs on each virtual bond τ_2 , there will be four Majorana fermions at each physical index μ_2 with the following properties under D_2 symmetry:

$$\begin{aligned} \mathbf{M}_1 : (\gamma_1, \gamma'_1, \gamma_2, \gamma'_2) &\mapsto (\gamma'_1, \gamma_1, \gamma'_2, \gamma_2) \\ \mathbf{M}_2 : (\gamma_1, \gamma'_1, \gamma_2, \gamma'_2) &\mapsto (\gamma_2, \gamma'_2, \gamma_1, \gamma'_1) \end{aligned} \quad (19)$$

Here \mathbf{M}_1 and \mathbf{M}_2 are two reflection generators of D_2 with horizontal and vertical axes, respectively. Define two complex fermions from these 4 Majorana fermions, with D_2 symmetry properties:

$$\begin{cases} c_1^\dagger = \frac{1}{2}(\gamma_1 + i\gamma'_1) \\ c_2^\dagger = \frac{1}{2}(\gamma_2 + i\gamma'_2) \end{cases}, \begin{cases} \mathbf{M}_1 : (c_1^\dagger, c_2^\dagger) \mapsto (ic_1, ic_2) \\ \mathbf{M}_2 : (c_1^\dagger, c_2^\dagger) \mapsto (c_2^\dagger, c_1^\dagger) \end{cases} \quad (20)$$

We denote the fermion number operators $n_1 = c_1^\dagger c_1$ and $n_2 = c_2^\dagger c_2$. Firstly we consider a Hamiltonian of Hubbard interaction ($U > 0$):

$$H_U = U \left(n_1 - \frac{1}{2} \right) \left(n_2 - \frac{1}{2} \right) \quad (21)$$

It is easy to verify that H_U respect the D_2 symmetry. There is a 2-fold ground-state degeneracy from $(n_1, n_2) = (1, 0)$ or $(0, 1)$ that can be viewed as a spin-1/2 degree of freedom:

$$\tau_{12}^\mu = \begin{pmatrix} c_1^\dagger & c_2^\dagger \end{pmatrix} \sigma^\mu \begin{pmatrix} c_1 \\ c_2 \end{pmatrix} \quad (22)$$

In order to investigate that whether the degenerate ground states can be gapped out, we focus on the projective Hilbert space spanned by two states $c_1^\dagger|0\rangle$ and $c_2^\dagger|0\rangle$. In this projective Hilbert space, $\mathbf{M}_1 = \sigma^y$ and $\mathbf{M}_2 = \sigma^x$ and they are anticommuting:

$$\mathbf{M}_1 \mathbf{M}_2 = -\mathbf{M}_2 \mathbf{M}_1 \quad (23)$$

Thus the projective Hilbert space is a projective representation of the D_2 group. Accordingly, the double MEPs on each virtual bond τ_2 is obstructed. Similar to the virtual bond τ_3 , and they are obstructed.

There is one exception: if there are double MEPs on both τ_2 and τ_3 , there are two copies of the aforementioned projective representations of D_2 on each physical bond μ_2 or μ_3 . They can form a linear representation of D_2 because there is only one nontrivial projective representation of D_2 guaranteed by the 2-cohomology $\mathcal{H}^2[D_2, U(1)] = \mathbb{Z}_2$. As the consequence, this exception is obstruction-free. We claim that it can only be

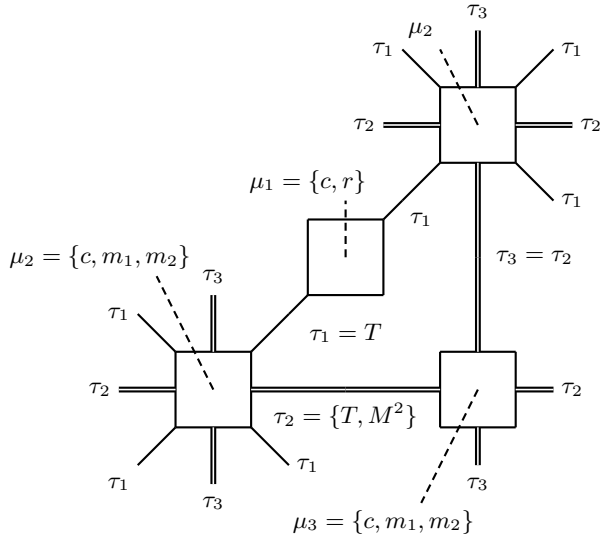


FIG. 5. All obstruction-free PEPS tensors in a unit cell of cmm -symmetric lattice for spinless fermions. Here t/T represents the trivial physical/virtual index, M^2 represents the double MEPs, and the virtual indices τ_2 and τ_3 should be identical.

obstruction-free with interactions, otherwise it is still obstructed.

Summarize above discussions, all obstruction-free PEPS tensors form a \mathbb{Z}_2^9 group, \mathbb{Z}_2^8 is from the physical indices μ_1 , μ_2 , and μ_3 , and the remaining \mathbb{Z}_2 is from the double MEPs on virtual bonds τ_2 and τ_3 . All obstruction-free PEPS tensors in a unit cell are illustrated in Fig. 5.

Next, we investigate the possible trivializations of the PEPS tensors. There are several possibilities:

1. We have demonstrated that there is no nontrivial and obstruction-free virtual index on τ_1 . Nevertheless, there is a subtlety that both vacuum and entanglement pair of two complex fermions on τ_1 are trivial virtual indices [$n_1 = 0$ in Eq. (13) with $G_{\tau_1} = 0$], but they give different physical indices μ_1 : the former case leaves nothing on all physical indices, but the later case leaves two complex fermions c_1^\dagger, c_2^\dagger on the physical index μ_1 forming an atomic insulator $|\psi\rangle_{\mu_1} = c_1^\dagger c_2^\dagger |0\rangle$ and four complex fermions c_j^\dagger ($j = 1, 2, 3, 4$) on the physical index μ_2 forming another atomic insulator $|\psi\rangle_{\mu_2} = c_1^\dagger c_2^\dagger c_3^\dagger c_4^\dagger |0\rangle$, with the following symmetry properties:

$$\begin{aligned} \mathbf{R}|\psi\rangle_{\mu_1} &= c_2^\dagger c_1^\dagger |0\rangle = -|\psi\rangle_{\mu_1} \\ \mathbf{M}_1|\psi\rangle_{\mu_2} &= c_2^\dagger c_1^\dagger c_4^\dagger c_3^\dagger |0\rangle = |\psi\rangle_{\mu_2} \\ \mathbf{M}_2|\psi\rangle_{\mu_2} &= c_4^\dagger c_3^\dagger c_2^\dagger c_1^\dagger |0\rangle = |\psi\rangle_{\mu_2} \end{aligned} \quad (24)$$

i.e., $|\psi\rangle_{\mu_1}$ represents the state of eigenvalue -1 under 2-fold rotation symmetry, labeled by r . On the other hand, by definition, the PEPS tensors within one unit cell $\bigoplus_{j=1}^3 A_{\mu_j}$ should be an injective map from connect-

ing virtual indices to a physical indices (injective condition), hence the atomic insulator $|\psi\rangle_{\mu_1}$ corresponds to trivial physical index at μ_1 . Equivalently, the physical index r at μ_1 is *trivialized*.

2. Similar to above case, both vacuum and entanglement pair of two complex fermions on τ_2 are trivial virtual indices [$n_1 = 0$ in Eq. (13) with $G_{\tau_2} = \mathbb{Z}_2$], but give different physical indices μ_2 and μ_3 : the former case leaves nothing on all physical indices, but the later case leaves two complex fermions on the physical index μ_2 forming an atomic insulator $|\phi\rangle_{\mu_2} = c_1^\dagger c_2^\dagger |0\rangle$ and two complex fermions on the physical index μ_3 forming another atomic insulator $|\phi\rangle_{\mu_3} = c_1^\dagger c_2^\dagger |0\rangle$. Under vertical reflection \mathbf{M}_2 :

$$\begin{aligned} \mathbf{M}_2|\phi\rangle_{\mu_2} &= c_2^\dagger c_1^\dagger |0\rangle = -|\phi\rangle_{\mu_2} \\ \mathbf{M}_2|\phi\rangle_{\mu_3} &= c_2^\dagger c_1^\dagger |0\rangle = -|\phi\rangle_{\mu_3} \end{aligned} \quad (25)$$

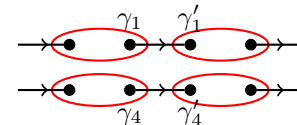
i.e., $|\phi\rangle_{\mu_2, \mu_3}$ represents the state with eigenvalue -1 of \mathbf{M}_2 , labeled by m_2 . According to the injective condition of the PEPS tensors within one unit cell, the atomic insulators $|\phi\rangle_{\mu_2}$ and $|\phi\rangle_{\mu_3}$ together correspond to trivial physical indices at μ_2 and μ_3 . Equivalently, the physical indices m_2 at both μ_2 and μ_3 are trivialized.

3. Repeatedly, both vacuum and entanglement pair of two complex fermions on τ_3 are trivial virtual indices, but give different physical indices μ_2 and μ_3 : the former case leaves nothing on all physical indices, but the later case leaves two complex fermions on the physical index μ_2 forming an atomic insulator $|\eta\rangle_{\mu_2} = c_1^\dagger c_2^\dagger |0\rangle$ and two complex fermions on the physical index μ_3 forming another atomic insulator $|\eta\rangle_{\mu_3} = c_1^\dagger c_2^\dagger |0\rangle$. Under horizontal reflection \mathbf{M}_1 :

$$\begin{aligned} \mathbf{M}_1|\eta\rangle_{\mu_2} &= c_2^\dagger c_1^\dagger |0\rangle = -|\eta\rangle_{\mu_2} \\ \mathbf{M}_1|\eta\rangle_{\mu_3} &= c_2^\dagger c_1^\dagger |0\rangle = -|\eta\rangle_{\mu_3} \end{aligned} \quad (26)$$

i.e., $|\eta\rangle_{\mu_2, \mu_3}$ represents the state of eigenvalue -1 of \mathbf{M}_1 , labeled by m_1 . According to the injective condition of the PEPS tensors within one unit cell, the atomic insulators $|\eta\rangle_{\mu_2}$ and $|\eta\rangle_{\mu_3}$ together correspond to trivial physical indices at μ_2 and μ_3 . Equivalently, the physical indices m_1 at both μ_2 and μ_3 are trivialized.

4. Again, both vacuum and double MEPs on τ_1 are trivial virtual indices, but give different physical indices μ_1 : the former case leaves nothing on all physical indices, but for the latter case, double MEPs can be illustrated as:



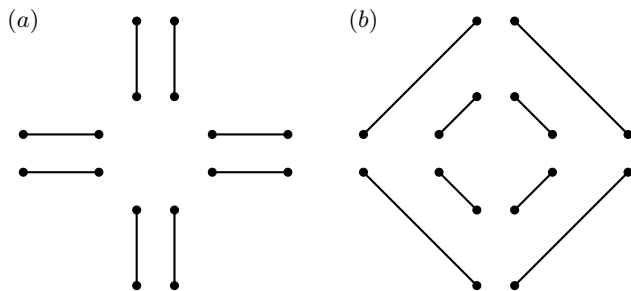
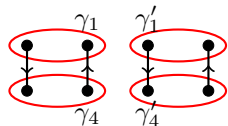


FIG. 6. Deformation of double MEPs on each virtual bond μ_2/μ_3 . (a)/(b) is the state before/after deformation, respectively. Here each black dot represents a Majorana fermion and each solid line represents an MEP.

Where the red ellipses represent the physical bonds and the arrows represent the Majorana entanglement pairs. Consider the Hamiltonian with a parameter θ :

$$H(\theta) = \cos \theta (-i\gamma_1\gamma'_1 - i\gamma_4\gamma'_4) + \sin \theta (i\gamma_1\gamma_4 - i\gamma'_1\gamma'_4) \quad (27)$$

The eigenvalues of $H(\theta)$ are independent with θ , hence the topological properties of $H(\theta)$ keep invariant for different parameter θ . In particular, $\theta = 0$ corresponds to two Majorana entanglement pairs and $\theta = \pi/2$ corresponds to the disentangled state with the form:



An important issue is that in this disentangled state, there is a Majorana chain with the periodic boundary condition (PBC) surrounding each lattice site μ . It is well-known that the fermion parity of the Majorana chain with PBC is odd [16], hence the double MEPs on each τ_1 leaves a fermion parity odd state on each physical index μ_1 .

On the other hand, consider double MEPs on each virtual bond τ_2/τ_3 illustrated as Fig. 6(a). We have demonstrated that this block-state is obstruction-free. Repeatedly apply the disentangling Hamiltonian (27), it can be deformed to Fig. 6(b) with double MEPs on each virtual bond τ_1 , as the above case that has been deformed to Majorana chains with PBCs surrounding 0D blocks labeled by μ_1 . Furthermore, we should identify that 8 Majorana fermions on each physical index μ_2/μ_3 are bound by interactions, hence they do not form a Majorana chain with PBC that can change the fermion parity of the corresponding physical index. As the consequence, the PEPS tensors with physical index c at each μ_1 and double MEPs on each τ_2/τ_3 are trivIALIZED.

To summarize these trivialisations, we conclude that the trivIALIZED non-vacuum PEPS tensors form a \mathbb{Z}_2^4 group.

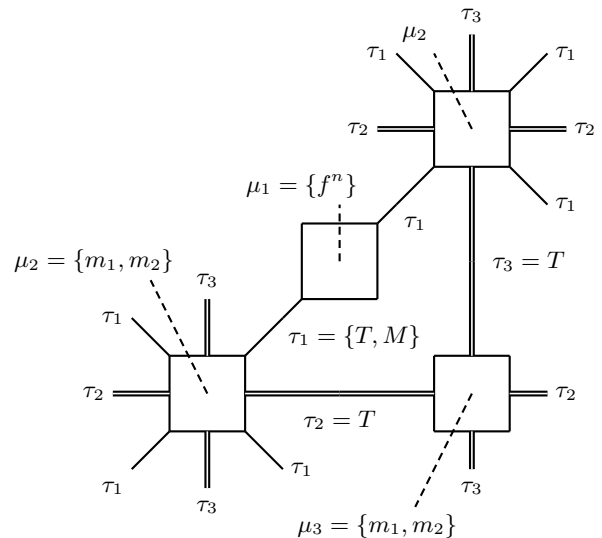


FIG. 7. All obstruction free PEPS tensors in a unit cell of *cmm*-symmetric lattice for spin-1/2 fermions. Here M represents the MEP, t/T represents the trivial physical/virtual index and $n = 0, 1, 2, 3$.

As the consequence, the ultimate classification for spinless fermions on 2D lattice with *cmm* symmetry is (the superscript represents the spin of fermions):

$$\mathcal{G}_{cmm}^0 = \mathbb{Z}_2^5 \quad (28)$$

B. Spin-1/2 fermions

Firstly we investigate the physical indices of A_{μ_j} ($j = 1, 2, 3$) that are characterized by Eqs. (16) and (17). Dimension of the physical index of A_{μ_1} is $d_1 = 4$ with one generator f characterizing the eigenvalues of \mathbb{Z}_4^f , satisfying $f^4 = 1$; dimension of the physical index of A_{μ_2}/A_{μ_3} is $d_{2,3} = 4$ with two generators: eigenvalue -1 of \mathbf{M}_1 and \mathbf{M}_2 (m_1 and m_2).

Subsequently we investigate the virtual indices τ_k ($k = 1, 2, 3$) that are characterized by Eqs. (13) and (14). Dimension of τ_1 is $D_1 = 2$ with one generator: MEP; dimension of $\tau_{2,3}$ is $D_{2,3} = 1$.

It is straightforward to verify that there is no obstruction and trivIALIZATION. Hence all obstruction and trivIALIZATION free PEPS tensors are illustrated in Fig. 7. We should further consider the group structure of the classification: As aforementioned, double MEPs on each τ_1 is a trivial virtual index but changes the fermion parity of the physical index τ_1 . It provides a composite rule of PEPS tensors that two copies of MEP on each τ_1 leads to a complex fermion on each μ_1 (see Fig. 8).

This composite rule indicates that there is a nontrivial stacking between physical indices and virtual indices that leads to a nontrivial group extension of the classification, characterized by the following short exact sequence (see

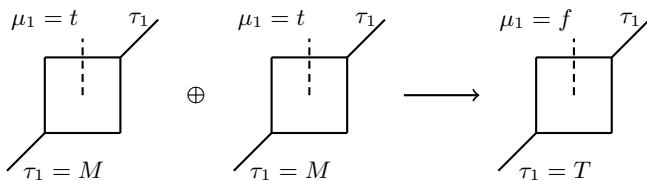


FIG. 8. Composite rule of the PEPS tensors A_{μ_1} . “ T ” represents the trivial virtual index, “ t ” represents the trivial physical index, “ M ” represents the MEP as the virtual index, and “ f ” represents the physical index with odd fermion parity.

Appendix A for more details):

$$0 \rightarrow \mathbb{Z}_2 \rightarrow \mathbb{Z}_8 \times \mathbb{Z}_2^4 \rightarrow \mathbb{Z}_4 \times \mathbb{Z}_2^4 \rightarrow 0 \quad (29)$$

Finally, the ultimate classification of the crystalline SPT phases with spin-1/2 fermions on the lattice with $cm\bar{m}$ symmetry is:

$$\mathcal{G}_{cm\bar{m}}^{1/2} = \mathbb{Z}_8 \times \mathbb{Z}_2^4 \quad (30)$$

V. CONCLUSION AND DISCUSSION

In this work, we establish the tensor-network representation of 2D crystalline fSPT phases and derive the classification by investigating the various degrees of freedom of PEPS tensors per unit cell. For a 2D lattice with a specific wallpaper group symmetry, we first put a PEPS tensor defined as a map from the connecting virtual indices to the physical index [cf. Eq. (2)] on each lattice site, whose physical and virtual indices have graded structure representing the fermion parity of the corresponding degrees of freedom. To describe the 2D crystalline fSPT phases, the PEPS tensors within a unit cell should be injective. Distinct from the SPT phases with on-site symmetry, the effective “on-site” symmetry (by crystalline symmetry acting internally) of the physical and virtual indices of PEPS tensors for describing the crystalline fSPT phases, G_p and G_v , might be different.

Then the symmetry properties of the PEPS tensors are shown in Eqs. (7) and (8), where U is the linear representation of G_p and V is the fMPO defined on the virtual indices crossing the edge of the regime under investigation. A partial classification might be from the F -moves and super pentagon equations of the fMPOs with graded structure. Nevertheless, we have elucidated that fMPOs do not contribute nontrivial 2D crystalline fSPT phases with wallpaper group symmetry via Eq. (12). In addition, due to the presence of the translation symmetry, the contributions from virtual and physical indices should also be taken into account, because the tensor renormalization procedure breaks the translation symmetry. The contributions from virtual indices are characterized by Eqs. (13) and (14), and the contributions from physical indices are characterized by Eqs. (16) and (17), and they form the classification data together.

G_b	spinless	spin-1/2
$p1$	$\mathbb{Z}_2 \times \mathbb{Z}_4$	$\mathbb{Z}_2 \times \mathbb{Z}_4$
$p2$	\mathbb{Z}_2^4	$\mathbb{Z}_4 \times \mathbb{Z}_8^3$
pm	\mathbb{Z}_2^6	$\mathbb{Z}_4 \times \mathbb{Z}_8$
pg	$\mathbb{Z}_2 \times \mathbb{Z}_4$	$\mathbb{Z}_4 \times \mathbb{Z}_2$
cm	\mathbb{Z}_2^4	$\mathbb{Z}_2 \times \mathbb{Z}_4$
pmm	\mathbb{Z}_2^8	\mathbb{Z}_2^8
pmg	\mathbb{Z}_2^5	$\mathbb{Z}_4 \times \mathbb{Z}_8^2$
pgg	\mathbb{Z}_2^3	$\mathbb{Z}_2 \times \mathbb{Z}_4 \times \mathbb{Z}_8$
$cm\bar{m}$	\mathbb{Z}_2^5	$\mathbb{Z}_8 \times \mathbb{Z}_2^4$
$p4$	$\mathbb{Z}_2^3 \times \mathbb{Z}_4$	$\mathbb{Z}_2 \times \mathbb{Z}_8^3$
$p4m$	\mathbb{Z}_2^7	\mathbb{Z}_2^6
$p4g$	\mathbb{Z}_2^4	$\mathbb{Z}_8 \times \mathbb{Z}_2^3$
$p3$	$\mathbb{Z}_2 \times \mathbb{Z}_3^3$	$\mathbb{Z}_2 \times \mathbb{Z}_3^3$
$p3m1$	\mathbb{Z}_2^3	\mathbb{Z}_4
$p31m$	$\mathbb{Z}_2^3 \times \mathbb{Z}_3$	$\mathbb{Z}_4 \times \mathbb{Z}_3$
$p6$	$\mathbb{Z}_2^2 \times \mathbb{Z}_3^2$	$\mathbb{Z}_{12} \times \mathbb{Z}_8 \times \mathbb{Z}_3$
$p6m$	\mathbb{Z}_2^4	\mathbb{Z}_2^4

TABLE I. Classifications for 2D crystalline fSPT phases protected by wallpaper group symmetry from tensor network representations, for both spinless and spin-1/2 fermions.

Subsequently, the possible obstructions and trivializations should be taken into account. By definition, the PEPS tensors defined in a unit cell should be an injective map from virtual indices to physical indices. If the connecting virtual indices of a PEPS tensor cannot be mapped to a valid physical index (i.e., a linear representation of G_p), we call the corresponding PEPS tensor is *obstructed*; with the condition of the injectivity, the physical indices shaped differently which are mapped from the same virtual indices should be equivalent.

Finally, by investigating the composite rule of different PEPS tensors, we can calculate the accurate group structure of the classification of 2D crystalline fSPT phases with wallpaper group symmetry. All results of classifications for both spinless and spin-1/2 fermions are summarized in Table I, and the corresponding PEPS tensors for all wallpaper groups within one unit cell are summarized in Figs. 9 and 10. Here we use single/double solid lines to label the virtual indices lying on/away from the reflection axis, equivalently, the effective on-site symmetry groups of virtual bonds labeled by single/double solid lines are $\mathbb{Z}_1/\mathbb{Z}_2$. All results are confirmed with our previous works in which the crystalline fSPT phases with wallpaper group symmetry were constructed and classified by real-space constructions [87].

Tensor network representation of 2D crystalline fSPT phases provides a powerful tool for investigating various problems of crystalline topological phases. For instance, consider a 2D lattice with a specific wallpaper group SG , and jointly protected by an on-site symmetry group G_0 , i.e., the total symmetry group of this lattice is $SG \times G_0$. The tensor network representation can also be applied to

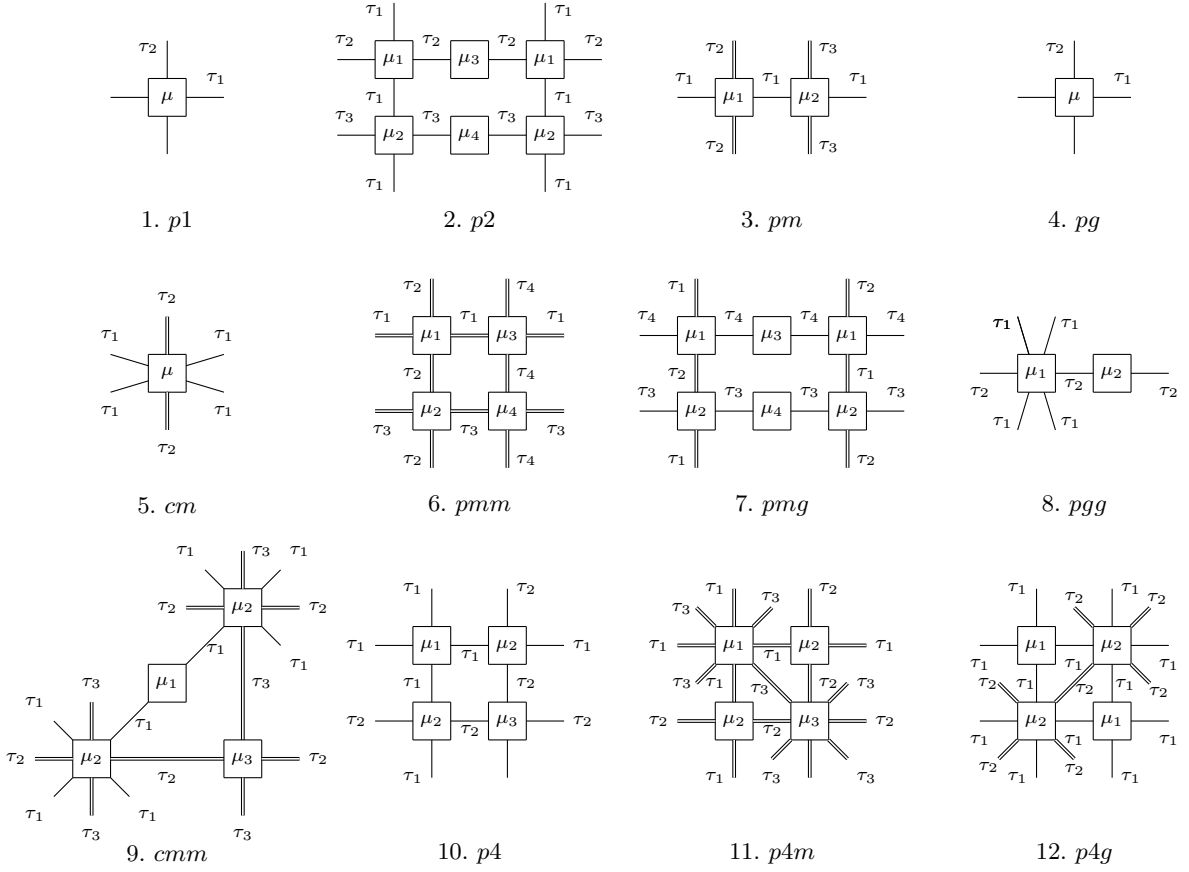


FIG. 9. The corresponding PEPS tensors for #1 to #12 wallpaper groups. Here μ 's label different physical indices, and τ 's label different virtual indices.

calculate the classification: the total on-site symmetry of physical/virtual indices are $G_0 \times G_p/G_0 \times G_v$, and the classification data is from the following species:

1. F -moves and super pentagon equations of fMPOs (the corresponding symmetry group is G_0);
2. Virtual indices, characterized by Eqs. (13) and (14);
3. Physical indices, characterized by Eqs. (16) and (17).

Then by investigating the obstruction, trivialization, and group structure as demonstrated in this paper, one can similarly obtain the classification of 2D fSPT phases jointly protected by crystalline and internal symmetries.

Furthermore, Tensor network is one of the most powerful tools to investigate the topological phase transition, hence based on this work, by constructing the explicit PEPS ground state wavefunctions, the topological phase transition between different crystalline fSPT phases can be investigated under their tensor network representations.

ACKNOWLEDGMENTS

We thank Zheng-Cheng Gu and Rui-Xing Zhang for enlightening discussions. JHZ is supported by Direct Grant No. 4053409 from The Chinese University of Hong Kong and funding from Hong Kong's Research Grants Council (GRF No.14306918, ANR/RGC Joint Research Scheme No. A-CUHK402/18). SY is supported by NSFC (Grant No. 11804181, No. 12174214) and the National Key R&D Program of China (Grant No. 2018YFA0306504).

Appendix A: Group extension, the spin of fermions and short exact sequence

In the main text, we have discussed the tensor network states of 2D crystalline fSPT phases for both spinless and spin-1/2 fermions, and the group structure of the classification characterized by possible nontrivial extensions between virtual and physical indices. In this section, we discuss the mathematical foundation of these issues: the short exact sequence.

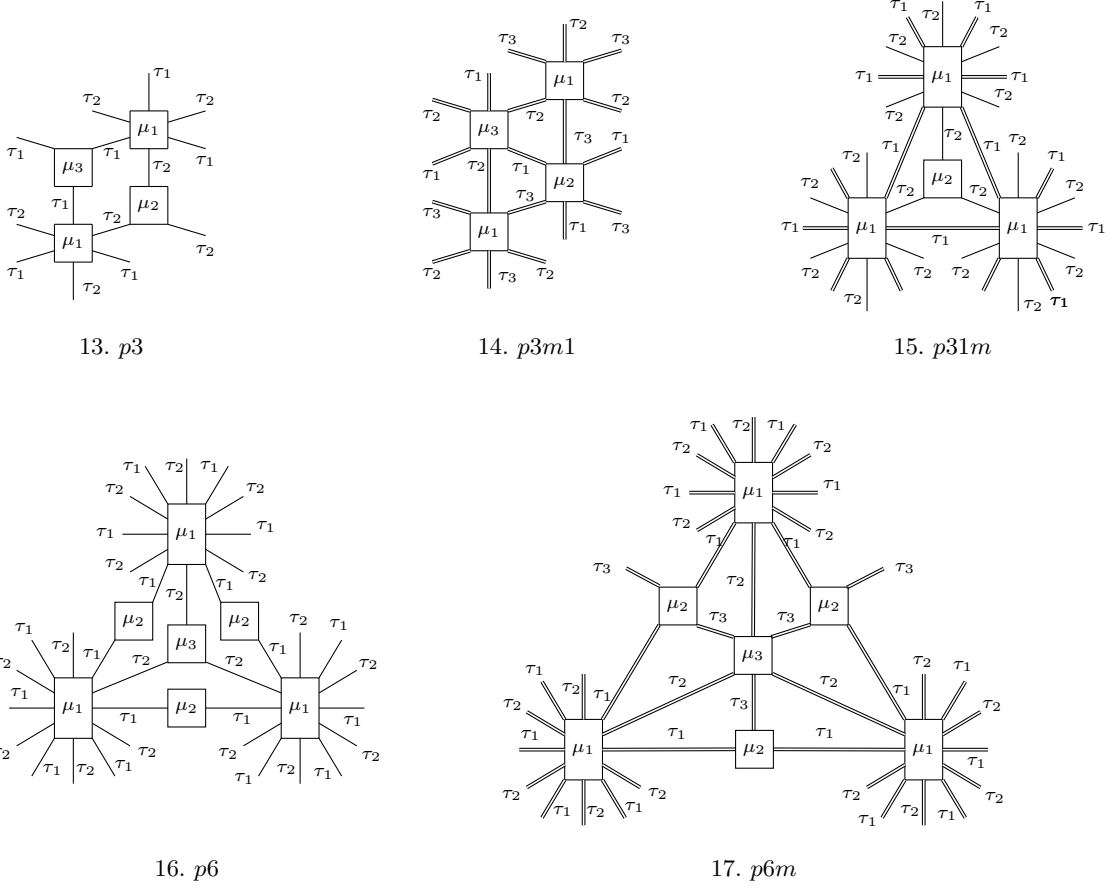


FIG. 10. The corresponding PEPS tensors for #13 to #17 wallpaper groups. Here μ 's label different physical indices, and τ 's label different virtual indices.

1. Central extension of groups

The following issues are characterized by different group extensions:

1. The spin of fermions (spinless or spin-1/2) are characterized by different central extensions of fermion parity \mathbb{Z}_2^f by the physical symmetry group G_b :

$$0 \rightarrow \mathbb{Z}_2^f \rightarrow G_f \rightarrow G_b \rightarrow 0 \quad (\text{A1})$$

different central extensions are characterized by different factor systems $\omega_2 \in \mathcal{H}^2(G_b, \mathbb{Z}_2)$.

2. The group structure of the classification is central extension of degrees of freedom of virtual indices by physical indices.

a. Lemma (Factor system) For a group (G, \cdot) , an Abelian group $(A, +)$, and a short exact sequence:

$$0 \rightarrow A \rightarrow X \rightarrow G \rightarrow 0 \quad (\text{A2})$$

There is a factor system of the short exact sequence Eq. (A2) who consists the function f and a homomorphism

σ :

$$\begin{aligned} f : G \times G &\longrightarrow A & \sigma : G &\longrightarrow \text{End}(A) \\ (g, h) &\longmapsto f(g, h) & g &\longmapsto \sigma_g \end{aligned} \quad (\text{A3})$$

where $\text{End}(A)$ is the endomorphism of the Abelian group A . such that it makes the Cartesian product $G \times A$ a group X with multiplication:

$$(g, a) * (h, b) = (g \cdot h, f(g, h) + a + \sigma_g(b)) \quad (\text{A4})$$

And f must be a group 2-cocycle which is classified by 2 group cohomology: $f \in \mathcal{H}^2(G, A)$. Where $\text{End}(A)$ is the endomorphism of group A .

2. Physical understanding of spin of fermions

From quantum mechanics, we know that for a fermion with well-defined spin, it should be an eigenstate of the spin angular momentum operator \hat{S}_z with a well defined magnetic quantum number σ_z : $\sigma_z = 0$ for spinless fermion and $\sigma_z = 1/2$ for spin-1/2 fermion, with eigen-wavefunction proportional to the phase factor $e^{i\sigma_z\phi}$, $\phi \in [0, 2\pi)$. For spinless fermions, if we rotate it by a lap

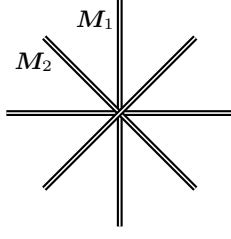


FIG. 11. Two independent reflection axes as two generators of D_4 symmetry.

(i.e., change ϕ from 0 to 2π), there is nothing changed because $\sigma_z = 0$; for spin-1/2 fermions, if we rotate it by a lap, the phase factor $e^{i\sigma_z\phi}$ is changed by -1 . They can be properly characterized by different factor systems ω_2 of the short exact sequence (A1).

For example, consider even-fold dihedral group D_{2n} symmetry with two generators \mathbf{R} (rotation) and \mathbf{M} (reflection) satisfying $\mathbf{R}^{2n} = \mathbf{M}^2 = I$ ($n = 1, 2, 3$ and I is identity). Different extensions of fermion parity are characterized by different 2-cocycles ω_2 :

$$\omega_2 \in \mathcal{H}^2(D_{2n}, \mathbb{Z}_2) = \mathbb{Z}_2^3 \quad (\text{A5})$$

In particular, the spinless fermions corresponding to the trivial 2-cocycle ω_2 satisfying:

$$\mathbf{R}^{2n} = 1, \quad \mathbf{M}^2 = 1 \quad (\text{A6})$$

while the spin-1/2 fermions corresponding to the 2-cocycle ω_2 satisfying (P_f is the fermion parity operator):

$$\mathbf{R}^{2n} = \mathbf{M}^2 = P_f, \quad \mathbf{M}\mathbf{R}\mathbf{M}^{-1}\mathbf{R} = 1 \quad (\text{A7})$$

Appendix B: Physical indices in 2D systems

For a 2D lattice with arbitrary wallpaper group symmetry, a PEPS tensor should be aligned at the center of a specific 2D point group. In Sec. III we have demonstrated that the physical index of a specific PEPS tensor is characterized by 1D irreducible representation of the *total* symmetry group G_f , and classified by group 1-cohomology $\mathcal{H}^1[G_f, U(1)]$. We identify all possible physical indices of PEPS tensors aligned at the center of 2D point groups.

We demonstrate the 4-order dihedral group D_4 as an example, and all other possibilities are summarized in Tables II and III.

For spinless fermions, different 1D irreducible representations of the total symmetry group $\mathbb{Z}_2^f \times D_4$ are classified by group 1-cohomology [93, 94]:

$$\mathcal{H}^1 \left[\mathbb{Z}_2^f \times D_4, U(1) \right] = \mathbb{Z}_2^3 \quad (\text{B1})$$

Hence for spinless fermions, if we put a PEPS tensor at the center of D_4 symmetry, the dimension of corresponding physical index is $d = 8$, with three generators: c

point group	dimension	generator
C_1	$d = 2$	$\{c\}$
C_2	$d = 4$	$\{c, r r^2 = 1\}$
C_3	$d = 6$	$\{c, r r^3 = 1\}$
C_4	$d = 8$	$\{c, r r^4 = 1\}$
C_6	$d = 12$	$\{c, r r^6 = 1\}$
D_1	$d = 4$	$\{c, m m^2 = 1\}$
D_2	$d = 8$	$\{c, m_1, m_2 m_1^2 = m_2^2 = 1\}$
D_3	$d = 4$	$\{c, m m^2 = 1\}$
D_4	$d = 8$	$\{c, m_1, m_2 m_1^2 = m_2^2 = 1\}$
D_6	$d = 8$	$\{c, m_1, m_2 m_1^2 = m_2^2 = 1\}$

TABLE II. Physical indices of PEPS tensors located at centers of 2D point groups for spinless fermions, including their dimensions and generators. Here c labels the complex fermion, r labels the rotation eigenvalues and $m/m_1/m_2$ labels different reflection eigenvalues.

point group	dimension	generator
C_1	$d = 2$	$\{c\}$
C_2	$d = 4$	$\{f^n n = 0, 1, 2, 3\}$
C_3	$d = 6$	$\{c, r r^3 = 1\}$
C_4	$d = 8$	$\{f^n n = 0, 1, \dots, 7\}$
C_6	$d = 12$	$\{f^n n = 0, 1, \dots, 11\}$
D_1	$d = 4$	$\{f^n n = 0, 1, 2, 3\}$
D_2	$d = 4$	$\{m_1, m_2 m_1^2 = m_2^2 = 1\}$
D_3	$d = 4$	$\{f^n n = 0, 1, 2, 3\}$
D_4	$d = 4$	$\{m_1, m_2 m_1^2 = m_2^2 = 1\}$
D_6	$d = 4$	$\{m_1, m_2 m_1^2 = m_2^2 = 1\}$

TABLE III. Physical indices of PEPS tensors located at centers of 2D point groups for spin-1/2 fermions, including their dimensions and generators. Here c labels the complex fermion, r labels the rotation eigenvalues, m_1/m_2 labels different reflection eigenvalues and f^n labels fermionic mode carries nontrivial eigenvalues of point group symmetry action.

labels the complex fermions, m_1 and m_2 label the eigenvalues -1 of two independent reflection generators \mathbf{M}_1 and \mathbf{M}_2 , of D_4 group (see Fig. 11).

For spin-1/2 fermions, different 1D irreducible representations of the total symmetry group $\mathbb{Z}_2^f \times_{\omega_2} D_4$ are classified by an alternative group 1-cohomology:

$$\mathcal{H}^1 \left[\mathbb{Z}_2^f \times_{\omega_2} D_4, U(1) \right] = \mathbb{Z}_2^2 \quad (\text{B2})$$

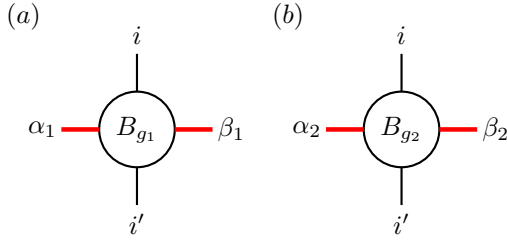
Hence for spin-1/2 fermions, if we put a PEPS tensor at the center of D_4 symmetry, the dimension of corresponding physical index is $d = 4$, with two generators: m_1 and m_2 label the eigenvalues -1 of two independent reflection generators \mathbf{M}_1 and \mathbf{M}_2 of D_4 group (see Fig. 11).

Appendix C: Superposition of MPOs with graded structure

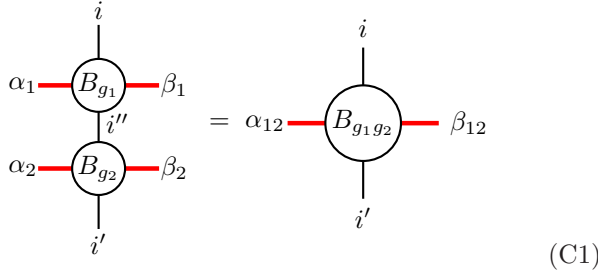
In this section, we review the superposition of MPOs for both bosonic (bMPO) and fermionic (fMPO) systems, and deduce the 3-cohomology structure from the F -move and pentagon equation. In particular, because of the super (graded) structure of the fermionic PEPS and fMPOs, the mathematical structure of the fMPOs is 3-order group super-cohomology [15–17].

1. Superposition of bMPOs

Consider the following two bMPOs with symmetry G ($g_1, g_2 \in G$):

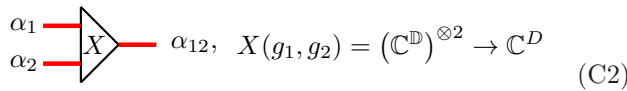


Multiplying the bMPOs B_{g_1} and B_{g_2} gives a new tensor $B_{g_1 g_2}$:



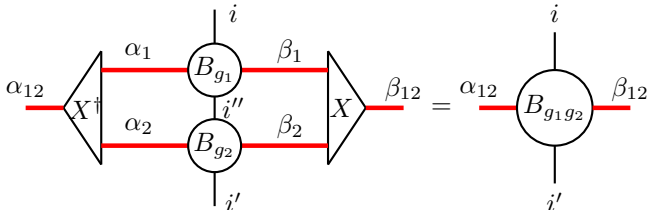
(C1)

Define a projection operator that can be illustrated graphically as:



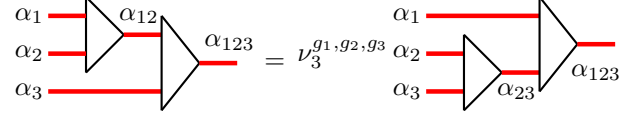
(C2)

Then the superposition rule [cf. Eq. (C1)] can be rephrased in terms of the projection operators:



a. Superpositions of three bMPOs: F -move

After defining the projection operator X , we are ready to consider the superpositions of three bMPOs: F -move. For three virtual indices α_j ($j = 1, 2, 3$), there are two different but equivalent ways of superposition: superpose $(\alpha_1, \alpha_2)/(\alpha_2, \alpha_3)$ first. Since the same bMPO will be obtained in two different ways, they can only differ by a $U(1)$ phase. Graphically:



where $\nu_3^{g_1, g_2, g_3} \in U(1)$ because in quantum mechanics, wavefunctions differ by a $U(1)$ phase characterize the same physical state. To further investigate the mathematical properties of this phase, we should consider the superpositions of more bMPOs.

b. Superpositions of four bMPOs: Pentagon equation

To investigate the aforementioned $U(1)$ phase $\nu_3^{g_1, g_2, g_3}$, we should consider the pentagon equation of the superpositions of four bMPOs, because there are several different but equivalent ways to superpose 4 bMPOs up to a $U(1)$ phase. Equivalently, we can investigate the mathematical structure of the $U(1)$ phase $\nu_3^{g_1, g_2, g_3}$. The pentagon equation can be represented graphically in Fig. 12.

From the pentagon equation we find the mathematical condition of the $U(1)$ phase ν_3 ($g_j \in G$, $j = 1, 2, 3, 4$):

$$d\nu_3(g_1, g_2, g_3, g_4) = \frac{\nu_3^{g_1, g_2, g_3} \nu_3^{g_1, g_2, g_3, g_4} \nu_3^{g_2, g_3, g_4}}{\nu_3^{g_1, g_2, g_3, g_4} \nu_3^{g_1, g_2, g_3, g_4}} = 1 \quad (\text{C3})$$

i.e., 3-cocycle condition. Equivalently, ν_3 is classified by 3-cohomology with $U(1)$ coefficient:

$$\nu_3 \in \mathcal{H}^3[G, U(1)] \quad (\text{C4})$$

Thus the superposition of bMPOs gives the 3-cohomology mathematical structure, hence the 2D bosonic symmetry-protected topological (bSPT) phases are classified by 3-cohomology with $U(1)$ coefficient [8, 9, 47].

2. Superposition of fMPOs

In the main text we have demonstrated that for arbitrary physical/virtual indices of a fermionic PEPS, there is an additional graded structure that describing the fermion parity. In addition, we should further identify the spin of fermions (spinless and spin-1/2) that is characterized by the extension of the physical symmetry

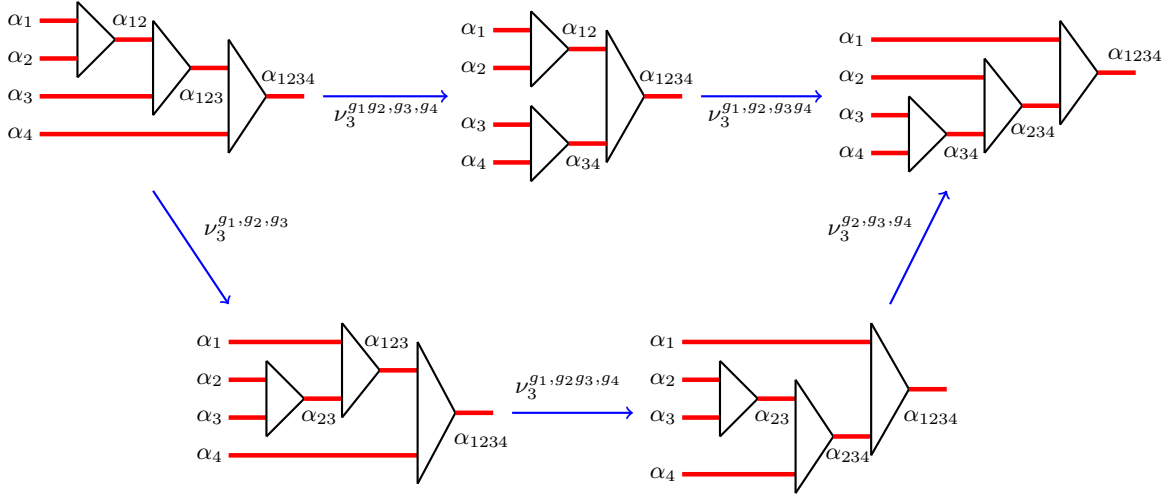


FIG. 12. The pentagon equation of superposing four bMPOs. Each step of F -move gives rise to a $U(1)$ phase.

group G_b by fermion parity \mathbb{Z}_2^f which is described by the following short-exact sequence:

$$0 \rightarrow \mathbb{Z}_2^f \rightarrow G_f \rightarrow G_b \rightarrow 0 \quad (\text{C5})$$

Spinless fermions is characterized by trivial 2-cocycle $\omega_2 = 0 \in \mathcal{H}^2(G_b, \mathbb{Z}_2)$, and the total symmetry group is labeled by $G_f = G_b \times \mathbb{Z}_2^f$; spin-1/2 fermions is characterized by nontrivial 2-cocycle $\omega_2 \in \mathcal{H}^2(G_b, \mathbb{Z}_2)$, and the total symmetry group is labeled by $G_f = G_b \times_{\omega_2} \mathbb{Z}_2^f$. Because all wallpaper group symmetry actions are unitary, we focus on the unitary symmetry groups exclusively.

Inherit from the graded structure of the PEPS, the graded structure of the indices of fMPOs is characterized by a map $n_2 : G_b \times G_b \rightarrow \mathbb{Z}_2$ and classified by 2-cohomology $\mathcal{H}^2(G_b, \mathbb{Z}_2)$, satisfying 2-cocycle condition (modulo 2, where $g_1, g_2, g_3 \in G_b$):

$$n_2(g_1, g_2) + n_2(g_1g_2, g_3) = n_2(g_1, g_2g_3) + n_2(g_2, g_3) \quad (\text{C6})$$

Similar to the PEPS tensor, the projection operator defined in Eq. (C2) should also be fermion parity even. Nevertheless, the fMPOs can be either even or odd of fermion parity.

We consider the PEPS tensors with even fMPOs first. The super F -move still gives rise to a $U(1)$ phase $\nu_3^{g_1, g_2, g_3}$. Nevertheless, because of the graded structure of the fMPOs, the super pentagon equation (see Fig. 12) gives the twisted 3-cocycle conditions. For spinless fermions, the super pentagon equation gives the relation as follows:

$$\frac{\nu_3^{g_1, g_2, g_3} \nu_3^{g_1, g_2, g_3, g_4} \nu_3^{g_2, g_3, g_4}}{\nu_3^{g_1, g_2, g_3, g_4} \nu_3^{g_1, g_2, g_3, g_4}} = (-1)^{n_2(g_1, g_2)n_2(g_3, g_4)} \quad (\text{C7})$$

where $n_2(g_1, g_2)n_2(g_3, g_4)$ can be labeled by cup product:

$$n_2(g_1, g_2)n_2(g_3, g_4) = n_2 \smile n_2(g_1, g_2, g_3, g_4)$$

For spin-1/2 fermions, the super pentagon equation gives the relation as following ($j = 1, 2, 3, 4$):

$$\frac{\nu_3^{g_1, g_2, g_3} \nu_3^{g_1, g_2, g_3, g_4} \nu_3^{g_2, g_3, g_4}}{\nu_3^{g_1, g_2, g_3, g_4} \nu_3^{g_1, g_2, g_3, g_4}} = (-1)^{(\omega_2 + n_2) \smile n_2(\{g_j\})} \quad (\text{C8})$$

where $\{g_j\} = g_1, g_2, g_3, g_4$. With this conditions, we notice that the 2D fermionic SPT (fSPT) phases with even fMPOs are classified by two indices (in the system without translation symmetry):

$$\begin{cases} n_2 \in \mathcal{H}^2(G_b, \mathbb{Z}_2) \\ \nu_3 \in \mathcal{H}^3[G_b, U(1)] \end{cases} \quad (\text{C9})$$

with the twisted 3-cocycle conditions [Eq. (C7) for spinless fermions, Eq. (C8) for spin-1/2 fermions].

The aforementioned fMPOs are fermion parity even, although the fermion parities of their physical or virtual indices might be odd. For fMPOs with odd fermion parity, there is an additional possibility: Majorana zero modes on ∂R that was missed in the previous discussions [54]. Equivalently, for this case, each virtual bond of the fermionic PEPS tensors represents the Majorana entanglement pair. The parity of the fMPOs that gives an additional index of the fSPT phases can be characterized by a map $n_1 : G_b \rightarrow \mathbb{Z}_2$ and classified by 1-cohomology with \mathbb{Z}_2 coefficient: $\mathcal{H}^1(G, \mathbb{Z}_2)$, satisfying ($g_1, g_2 \in G_b$):

$$n_1(g_1) + n_1(g_2) - n_1(g_1g_2) = 0 \quad (\text{C10})$$

Furthermore, the parity of fMPOs gives rise to an additional twist to the graded structure of the physical and virtual indices for spin-1/2 fermions, which is reflected in the 2-cocycle condition of n_2 ($g_1, g_2, g_3 \in G_b$):

$$\begin{aligned} n_2(g_1, g_2) + n_2(g_1g_2, g_3) - n_2(g_1, g_2g_3) - n_2(g_2, g_3) \\ = \omega_2 \smile n_1(g_1, g_2, g_3) \end{aligned} \quad (\text{C11})$$

Finally, we conclude that the 2D fSPT phases are classified by the following three indices (in the system without translation symmetry):

$$\begin{cases} n_1 \in \mathcal{H}^1(G_b, \mathbb{Z}_2) \\ n_2 \in \mathcal{H}^2(G_b, \mathbb{Z}_2) \\ \nu_3 \in \mathcal{H}^3[G_b, U(1)] \end{cases} \quad (\text{C12})$$

with the twisted cocycle conditions: Eqs. (C6) and (C7) for spinless fermions, Eqs. (C8) and (C11) for spin-1/2 fermions.

-
- [1] F. D. M. Haldane, “Nonlinear field theory of large-spin heisenberg antiferromagnets: Semiclassically quantized solitons of the one-dimensional easy-axis néel state,” *Phys. Rev. Lett* **50**, 1153 (1983).
- [2] Ian Affleck, Tom Kennedy, Elliott H. Lieb, and Hal Tasaki, “Rigorous results on valence-bond ground states in antiferromagnets,” *Phys. Rev. Lett.* **59**, 799 (1987).
- [3] M. Z. Hasan and C. L. Kane, “Colloquium: Topological insulators,” *Rev. Mod. Phys.* **82**, 3045–3067 (2010).
- [4] X.-L. Qi and S.-C. Zhang, “Topological insulators and superconductors,” *Rev. Mod. Phys.* **83**, 1057–1110 (2011).
- [5] F. Pollmann, A. M. Turner, E. Berg, and M. Oshikawa, “Entanglement spectrum of a topological phase in one dimension,” *Phys. Rev. B* **81**, 064439 (2010).
- [6] X. Chen, Z.-C. Gu, and X.-G. Wen, “Classification of gapped symmetric phases in one-dimensional spin systems,” *Phys. Rev. B* **83**, 035107 (2011).
- [7] X. Chen, Z.-C. Gu, and X.-G. Wen, “Complete classification of one-dimensional gapped quantum phases in interacting spin systems,” *Phys. Rev. B* **84**, 235128 (2011).
- [8] X. Chen, Z.-C. Gu, Z.-X. Liu, and X.-G. Wen, “Symmetry-protected topological orders in interacting bosonic systems,” *Science* **338**, 1604–1606 (2012).
- [9] X. Chen, Z.-C. Gu, Z.-X. Liu, and X.-G. Wen, “Symmetry protected topological orders and the group cohomology of their symmetry group,” *Phys. Rev. B* **87**, 155114 (2013).
- [10] Y.-M. Lu and A. Vishwanath, “Theory and classification of interacting integer topological phases in two dimensions: A chern-simons approach,” *Phys. Rev. B* **86**, 125119 (2012).
- [11] D. S. Freed, “Short-range entanglement and invertible field theories,” [arXiv:1406.7278 \[cond-mat.str-el\]](https://arxiv.org/abs/1406.7278).
- [12] Daniel S. Freed and Michael J. Hopkins, “Reflection positivity and invertible topological phases,” [arXiv e-prints \(2016\)](https://arxiv.org/abs/1604.06527), [arXiv:1604.06527](https://arxiv.org/abs/1604.06527).
- [13] A. Kapustin, “Symmetry protected topological phases, anomalies, and cobordisms: Beyond group cohomology,” [arXiv:1403.1467 \[cond-mat.str-el\]](https://arxiv.org/abs/1403.1467).
- [14] Xiao-Gang Wen, “Construction of bosonic symmetry-protected-trivial states and their topological invariants via $g \times so(\infty)$ nonlinear σ models,” *Phys. Rev. B* **91**, 205101 (2015).
- [15] Z.-C. Gu and X.-G. Wen, “Symmetry-protected topological orders for interacting fermions: Fermionic topological nonlinear σ models and a special group supercohomology theory,” *Phys. Rev. B* **90**, 115141 (2014).
- [16] Q.-R. Wang and Z.-C. Gu, “Towards a complete classification of symmetry-protected topological phases for interacting fermions in three dimensions and a general group supercohomology theory,” *Phys. Rev. X* **8**, 011055 (2018).
- [17] Q.-R. Wang and Z.-C. Gu, “Construction and classification of symmetry-protected topological phases in interacting fermion systems,” *Phys. Rev. X* **10**, 031055 (2020), [arXiv:1811.00536 \[cond-mat.str-el\]](https://arxiv.org/abs/1811.00536).
- [18] Anton Kapustin, Ryan Thorngren, Alex Turzillo, and Zitao Wang, “Fermionic symmetry protected topological phases and cobordisms,” *JHEP* **1512**, 052 (2015).
- [19] Anton Kapustin and Ryan Thorngren, “Fermionic spt phases in higher dimensions and bosonization,” *Journal of High Energy Physics* **2017**, 80 (2017).
- [20] Lukasz Fidkowski and Alexei Kitaev, “Effects of interactions on the topological classification of free fermion systems,” *Phys. Rev. B* **81**, 134509 (2010).
- [21] L. Fidkowski and A. Kitaev, “Topological phases of fermions in one dimension,” *Phys. Rev. B* **83**, 075103 (2011).
- [22] C. Wang, A. C. Potter, and T. Senthil, “Classification of Interacting Electronic Topological Insulators in Three Dimensions,” *Science* **343**, 629–631 (2014), [arXiv:1306.3238](https://arxiv.org/abs/1306.3238).
- [23] C. Wang and T. Senthil, “Interacting fermionic topological insulators/superconductors in three dimensions,” *Phys. Rev. B* **89**, 195124 (2014).
- [24] E. Witten, “Fermion path integrals and topological phases,” *Rev. Mod. Phys.* **88**, 035001 (2016).
- [25] M. Levin and Z.-C. Gu, “Braiding statistics approach to symmetry-protected topological phases,” *Phys. Rev. B* **86**, 115109 (2012).
- [26] Z.-C. Gu and M. Levin, “Effect of interactions on two-dimensional fermionic symmetry-protected topological phases with z_2 symmetry,” *Phys. Rev. B* **89**, 201113(R) (2014).
- [27] M. Cheng and Z.-C. Gu, “Topological response theory of abelian symmetry-protected topological phases in two dimensions,” *Phys. Rev. Lett.* **112**, 141602 (2014).
- [28] C. Wang and M. Levin, “Braiding statistics of loop excitations in three dimensions,” *Phys. Rev. Lett.* **113**, 080403 (2014).
- [29] S. Jiang, A. Mesaros, and Y. Ran, “Generalized modular transformations in (3 + 1)D topologically ordered phases and triple linking invariant of loop braiding,” *Phys. Rev. X* **4**, 031048 (2014).
- [30] J. C. Wang and X.-G. Wen, “Non-abelian string and particle braiding in topological order: Modular $SL(3, \mathbb{Z})$ representation and (3 + 1)-dimensional twisted gauge theory,” *Phys. Rev. B* **91**, 035134 (2015).
- [31] C. Wang and M. Levin, “Topological invariants for gauge theories and symmetry-protected topological phases,” *Phys. Rev. B* **91**, 165119 (2015).

- [32] C.-H. Lin and M. Levin, “Loop braiding statistics in exactly soluble three-dimensional lattice models,” *Phys. Rev. B* **92**, 035115 (2015).
- [33] M. Barkeshli, P. Bonderson, M. Cheng, and Z. Wang, “Symmetry fractionalization, defects, and gauging of topological phases,” *Phys. Rev. B* **100**, 115147 (2019), [arXiv:1410.4540 \[cond-mat.str-el\]](#).
- [34] N. Tantivasadakarn, “Dimensional reduction and topological invariants of symmetry-protected topological phases,” *Phys. Rev. B* **96**, 195101 (2017).
- [35] C. Wang, C.-H. Lin, and Z.-C. Gu, “Interacting fermionic symmetry-protected topological phases in two dimensions,” *Phys. Rev. B* **95**, 195147 (2017).
- [36] M. Cheng, Z. Bi, Y.-Z. You, and Z.-C. Gu, “Classification of symmetry-protected phases for interacting fermions in two dimensions,” *Phys. Rev. B* **97**, 205109 (2018).
- [37] M. Cheng, N. Tantivasadakarn, and C. Wang, “Loop braiding statistics and interacting fermionic symmetry-protected topological phases in three dimensions,” *Phys. Rev. X* **8**, 011054 (2018).
- [38] A. Vishwanath and T. Senthil, “Physics of three-dimensional bosonic topological insulators: Surface-deconfined criticality and quantized magnetoelectric effect,” *Phys. Rev. X* **3**, 011016 (2013).
- [39] C. Wang and T. Senthil, “Boson topological insulators: A window into highly entangled quantum phases,” *Phys. Rev. B* **87**, 235122 (2013).
- [40] X. Chen, F. J. Burnell, A. Vishwanath, and L. Fidkowski, “Anomalous symmetry fractionalization and surface topological order,” *Phys. Rev. X* **5**, 041013 (2015).
- [41] C. Wang, C.-H. Lin, and M. Levin, “Bulk-boundary correspondence for three-dimensional symmetry-protected topological phases,” *Phys. Rev. X* **6**, 021015 (2016).
- [42] P. Bonderson, C. Nayak, and X.-L. Qi, “A time-reversal invariant topological phase at the surface of a 3d topological insulator,” *Journal of Statistical Mechanics: Theory and Experiment* **2013**, P01016 (2013).
- [43] C. Wang, A. C. Potter, and T. Senthil, “Gapped symmetry preserving surface state for the electron topological insulator,” *Phys. Rev. B* **88**, 115137 (2013).
- [44] L. Fidkowski, X. Chen, and A. Vishwanath, “Non-abelian topological order on the surface of a 3d topological superconductor from an exactly solved model,” *Phys. Rev. X* **3**, 041016 (2013).
- [45] X. Chen, L. Fidkowski, and A. Vishwanath, “Symmetry enforced non-abelian topological order at the surface of a topological insulator,” *Phys. Rev. B* **89**, 165132 (2014).
- [46] F. Pollman, E. Berg, A. M. Turner, and M. Oshikawa, “Symmetry protection of topological phases in one-dimensional quantum spin systems,” *Phys. Rev. B* **85**, 075125 (2012).
- [47] X. Chen, Z.-X. Liu, and X.-G. Wen, “Two-dimensional symmetry-protected topological orders and their protected gapless edge excitations,” *Phys. Rev. B* **84**, 235141 (2011).
- [48] N. Schuch, D. Pérez-García, and I. Cirac, “Classifying quantum phases using matrix product states and projected entangled pair states,” *Phys. Rev. B* **84**, 165139 (2011).
- [49] T. B. Wahl, H.-H. Tu, N. Schuch, and J. I. Cirac, “Projected entangled-pair states can describe chiral topological states,” *Phys. Rev. Lett.* **111**, 236805 (2013).
- [50] Thorsten B. Wahl, Stefan T. Haßler, Hong-Hao Tu, J. Ignacio Cirac, and Norbert Schuch, “Symmetries and boundary theories for chiral projected entangled pair states,” *Phys. Rev. B* **90**, 115133 (2014).
- [51] J. Dubail and N. Read, “Tensor network trial states for chiral topological phases in two dimensions and a no-go theorem in any dimension,” *Phys. Rev. B* **92**, 205307 (2015).
- [52] Dominic J. Williamson, Nick Bultinck, Michael Mariën, Mehmet B. Sahinoglu, Jutho Haegeman, and Frank Verstraete, “Matrix product operators for symmetry-protected topological phases: Gauging and edge theories,” *Phys. Rev. B* **94**, 205150 (2016).
- [53] C. Wille, O. Buerschaper, , and J. Eisert, “Fermionic topological quantum states as tensor networks,” *Phys. Rev. B* **95**, 245127 (2017).
- [54] Nick Bultinck, Dominic J. Williamson, Jutho Haegeman, and Frank Verstraete, “Fermionic projected entangled-pair states and topological phases,” *J. Phys. A: Math. Theor.* **51**, 025202 (2017).
- [55] Andras Molnar, Yimin Ge, Norbert Schuch, and J. Ignacio Cirac, “A generalization of the injectivity condition for projected entangled pair states,” *J. Math. Phys.* **59**, 021902 (2018).
- [56] Anton Kapustin, Alex Turzillo, and Minyoung You, “Spin topological field theory and fermionic matrix product states,” *Phys. Rev. B* **98**, 125101 (2018).
- [57] Mehmet Burak Şahinoğlu, Dominic Williamson, Nick Bultinck, Michael Mariën, Jutho Haegeman, Norbert Schuch, and Frank Verstraete, “Characterizing topological order with matrix product operators,” *Ann. Henri Poincaré* **22**, 563–592 (2021).
- [58] L. Fu, “Topological crystalline insulators,” *Phys. Rev. Lett.* **106**, 106802 (2011).
- [59] T. H. Hsieh, H. Lin, J. Liu, W. Duan, A. Bansil, and L. Fu, “Topological crystalline insulators in the snt material class,” *Nat. Commun.* **3**, 982 (2012).
- [60] H. Isobe and L. Fu, “Theory of interlocking topological crystalline insulators,” *Phys. Rev. B* **92**, 081304(R) (2015).
- [61] H. Song, S.-J. Huang, L. Fu, and M. Hermele, “Topological phases protected by point group symmetry,” *Phys. Rev. X* **7**, 011020 (2017).
- [62] S.-J. Huang, H. Song, Y.-P. Huang, and M. Hermele, “Building crystalline topological phases from lower-dimensional states,” *Phys. Rev. B* **96**, 205106 (2017).
- [63] Ryan Thorngren and Dominic V. Else, “Gauging spatial symmetries and the classification of topological crystalline phases,” *Phys. Rev. X* **8**, 011040 (2018).
- [64] L. Zou, “Bulk characterization of topological crystalline insulators: Stability under interactions and relations to symmetry enriched u(1) quantum spin liquids,” *Phys. Rev. B* **97**, 045130 (2018).
- [65] H. C. Po, A. Vishwanath, and H. Watanabe, “Symmetry-based indicators of band topology in the 230 space groups,” *Nature Communications* **8**, 50 (2017).
- [66] H. Song, C. Z. Xiong, and S.-J. Huang, “Bosonic crystalline symmetry protected topological phases beyond the group cohomology proposal,” *Phys. Rev. B* **101**, 165129 (2020), [arXiv:1811.06558 \[cond-mat.str-el\]](#).
- [67] S. Jiang and Y. Ran, “Anyon condensation and a generic tensor-network construction for symmetry-protected topological phases,” *Phys. Rev. B* **95**, 125107 (2017).
- [68] J. Kruthoff, J. de Boer, J. van Wezel, C. L. Kane,

- and R.-J. Slager, “Topological classification of crystalline insulators through band structure combinatorics,” *Phys. Rev. X* **7**, 041069 (2017).
- [69] Ken Shiozaki, Masatoshi Sato, and Kiyonori Gomi, “Atiyah-hirzebruch spectral sequence in band topology: General formalism and topological invariants for 230 space groups,” [arXiv:1802.06694](https://arxiv.org/abs/1802.06694) [cond-mat.str-el].
- [70] Zhida Song, Sheng-Jie Huang, Yang Qi, Chen Fang, and Michael Hermele, “Topological states from topological crystals,” *Sci. Adv.* **5**, eaax2007 (2019), [arXiv:1810.02330](https://arxiv.org/abs/1810.02330) [cond-mat.mes-hall].
- [71] D. V. Else and R. Thorngren, “Crystalline topological phases as defect networks,” *Phys. Rev. B* **99**, 115116 (2019).
- [72] Z. Song, C. Fang, and Y. Qi, “Real-space recipes for general topological crystalline states,” *Nature Communications* **11**, 4197 (2020), [arXiv:1810.11013](https://arxiv.org/abs/1810.11013) [cond-mat.str-el].
- [73] Ken Shiozaki, Charles Zhaoxi Xiong, and Kiyonori Gomi, “Generalized homology and atiyah-hirzebruch spectral sequence in crystalline symmetry protected topological phenomena,” [arXiv:1810.00801](https://arxiv.org/abs/1810.00801) [cond-mat.str-el].
- [74] M. Cheng and C. Wang, “Rotation symmetry-protected topological phases of fermions,” [arXiv:1810.12308](https://arxiv.org/abs/1810.12308) [cond-mat.str-el].
- [75] Alex Rasmussen and Yuan-Ming Lu, “Classification and construction of higher-order symmetry protected topological phases of interacting bosons,” *Phys. Rev. B* **101**, 085137 (2020), [arXiv:1809.07325](https://arxiv.org/abs/1809.07325) [cond-mat.str-el].
- [76] A. Rasmussen and Y.-M. Lu, “Intrinsically interacting topological crystalline insulators and superconductors,” [arXiv:1810.12317](https://arxiv.org/abs/1810.12317) [cond-mat.str-el].
- [77] M. Cheng, “Fermionic lieb-schultz-mattis theorems and weak symmetry-protected phases,” *Phys. Rev. B* **99**, 075143 (2019).
- [78] S.-J. Huang and M. Hermele, “Surface field theories of point group symmetry protected topological phases,” *Phys. Rev. B* **97**, 075145 (2018).
- [79] S.-J. Huang, “4d beyond-cohomology topological phase protected by c_2 symmetry and its boundary theories,” *Phys. Rev. Research* **2**, 033236 (2020).
- [80] S.-J. Huang and Y.-T. Hsu, “Faithful derivation of symmetry indicators: A case study for topological superconductors with time-reversal and inversion symmetries,” *Phys. Rev. Research* **3**, 013243 (2021).
- [81] Zhengqiao Li Shang-Qiang Ning, Bin-Bin Mao and Chenjie Wang, “Anomaly indicators and bulk-boundary correspondences for three-dimensional interacting topological crystalline phases with mirror and continuous symmetries,” *Phys. Rev. B* (2021).
- [82] Y. Tanaka, Z. Ren, T. Sato, K. Nakayama, S. Souma, T. Takahashi, Kouji Segawa, and Yoichi Ando, “Experimental realization of a topological crystalline insulator in snte,” *Nature Physics* **8**, 800 (2012).
- [83] P. Dziawa, B. J. Kowalski, K. Dybko, R. Buczko, A. Szczerbakow, M. Szot, E. Lusakowska, T. Balasubramanian, B. M. Wojek, M. H. Berntsen, O. Tjernberg, and T. Story, “Topological crystalline insulator states in $\text{pb}_{1-x}\text{sn}_x\text{se}$,” *Nature Materials* **11**, 1023 (2012).
- [84] Y. Okada, M. Serbyn, H. Lin, D. Walkup, W. Zhou, C. Dhital, M. Neupane, S. Xu, Y. J. Wang, R. Sankar, F. Chou, A. Bansil, M. Z. Hasan, S. D. Wilson, L. Fu, and V. Madhavan, “Observation of dirac node formation and mass acquisition in a topological crystalline insulator,” *Science* **341**, 1496 (2013).
- [85] J. Ma, C. Yi, B. Lv, Z. Wang, S. Nie, L. Wang, L. Kong, Y. Huang, P. Richard, P. Zhang, K. Yaji, K. Kurado, S. Shin, H. Weng, B. A. Bernevig, Y. Shi, T. Qian, and H. Ding, “Experimental evidence of hourglass fermion in the candidate nonsymmorphic topological insulator khgsb ,” *Sci. Adv.* **3**, e1602415 (2017).
- [86] J.-H. Zhang, Q.-R. Wang, S. Yang, Y. Qi, and Z.-C. Gu, “Construction and classification of point-group symmetry-protected topological phases in two-dimensional interacting fermionic systems,” *Phys. Rev. B* **101**, 100501(R) (2020).
- [87] J.-H. Zhang, S. Yang, Y. Qi, and Z.-C. Gu, “Real-space construction of crystalline topological superconductors and insulators in 2d interacting fermionic systems,” [arXiv:2012.15657](https://arxiv.org/abs/2012.15657) [cond-mat.str-el].
- [88] Y. Ouyang, Q.-R. Wang, Z.-C. Gu, and Y. Qi, “Computing classification of interacting fermionic symmetry-protected topological phases using topological invariants,” [arXiv:2005.06572](https://arxiv.org/abs/2005.06572) [cond-mat.str-el].
- [89] M. F. Atiyah and F. Hirzebruch, *Topological Library: Part 3: Spectral Sequences in Topology* (World Scientific, 2003).
- [90] A. Kitaev, *Phys. Usp.* **44**, 131 (2001).
- [91] L. Fidkowski and A. Kitaev, *Phys. Rev. B* **83**, 075103 (2011).
- [92] For $G_v = 0$, the only one possible nontrivial dangling mode is Majorana zero mode; for $G_v = \mathbb{Z}_2$, there are two possible nontrivial dangling modes: Majorana zero mode and complex fermion.
- [93] GAP, “Gap - groups, algorithms, and programming, version 4.11.1,” <https://www.gap-system.org/> (2021).
- [94] G. Ellis, “Hap, homological algebra programming, version 1.28,” <http://hamilton.nuigalway.ie/Hap/www/> (2020).